J. Membrane Biol. 85, 25–35 (1985)

The Journal of
Membrane Biology

Vibrating Probe Analysis of Teleost Opercular Epithelium: Correlation between Active Transport and Leak Pathways of Individual Chloride Cells

J. Kevin Foskett* and Terry E. Machen
Departments of Zoology and Physiology-Anatomy, and Cancer Research Laboratory, University of California, Berkeley, California 94720

Summary. We have utilized the vibrating probe technique to examine transport by individual chloride cells in the short-circuited fish opercular epithelium. Variability in the steady state and in response to rapid perturbations, including fast-acting hormones and ion replacement, was analyzed. Negative short-circuit currents, corresponding to chloride secretion, were associated with the apical crypts of all but five of 386 chloride cells sampled. Average chloride cell short-circuit current and conductance were 2.7 ± 0.1 nA and 87.7 ± 3.8 nS, respectively, or 19 mA cm^{-2} and 620 mS cm^{-2} (resistance = 1.6 Ω cm^2) when normalized to apical crypt surface area. Exposure to 1 μM epinephrine rapidly inhibited the tissue short-circuit current by inhibiting the current pumped by all chloride cells, i.e. all chloride cells have adrenergic receptors. The time course of inhibition for each cell mirrored that of the whole tissue. Reversal of epinephrine inhibition of the tissue short-circuit current by glucagon and phosphodiesterase inhibition was by reversal of epinephrine's inhibition of individual chloride cells, and not by turning on cells which were previously inactive or uninhibited, or by stimulating nonchloride cells. A great amount of variability existed among chloride cells in the ability of these agents to reverse epinephrine-inhibited current. Likewise, considerable variability in the response of chloride cell conductance to these perturbations was observed, and in many instances a clear dissociation between current and conductance was noted. In the steady state, variability among cells in a single tissue always defined a linear relationship between chloride cell current and conductance with zero-current conductance intercept at zero. Equivalent circuit modeling indicates that the leak conductance of chloride cells within a single tissue always contributes the same proportion to the total individual chloride cell conductance, such that the ratio between the conductances of the active and leak pathways of chloride cells is constant. The leak pathway is almost certainly dominated by a sodium-selective paracellular pathway. The results suggest that these cells control the permeability of their paracellular pathway. A possible mechanism for this control is discussed.

Key Words extracellular recording · paracellular pathway · epinephrine · glucagon · chloride secretion · feedback

* *Present Address:* Laboratory of Kidney and Electrolyte Metabolism, National Heart, Lung and Blood Institute, Bldg. 10, Rm. 6N-307, National Institutes of Health, Bethesda, Md. 20205.

Introduction

Over the past 20 to 30 years, there has been interest in partitioning transepithelial electrophysiological parameters and ion and water flow between the transcellular and paracellular routes. Most epithelia are comprised of a heterogeneous population of cells, which complicates these efforts. In such tissues, one or more of the cell types may be involved in transepithelial transport, and each may be specialized for a specific transport function. As a result of heterogeneity, it is also desirable to assign and partition specific transport functions to specific cell types.

We recently adapted the vibrating probe technique to localize specific pathways for electrogenic transport and conductance in a heterogeneous epithelium, the fish opercular membrane (Foskett & Scheffey, 1982). The vibrating probe is a metal microelectrode which is rapidly vibrated between two points in the extracellular medium and allows measurement of the electric field along the line of vibration. It provides a low noise, low drift method for determining specific sites of localized current density immediately over the epithelial surface. We were able to localize peaks of negative current density over a single cell type, the chloride cell, which was consistent with the electrogenic chloride secretion capacity of the opercular membrane (Karnaky et al., 1977; Marshall & Bern, 1980; Foskett et al., 1981; 1982*a*; Foskett & Scheffey, 1982). In a subsequent report (Scheffey et al., 1983), refinements in the vibrating probe technique allowed localization of all transepithelial current flow and nearly all tissue-specific conductance to the apical crypts of chloride cells. As a result, it became possible to sample chloride cells with a spatial resolution of 5 μm and to determine the amount of short-circuit current and conductance for individual chloride

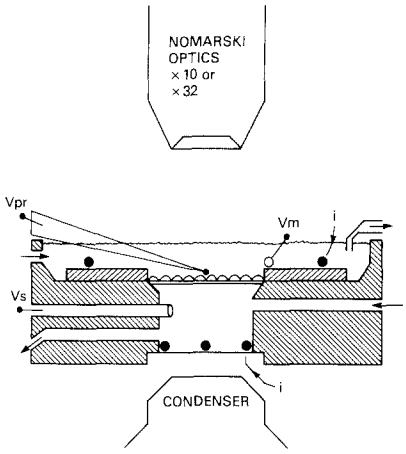

Fig. 1. Experimental set-up for vibrating probe (V_{pr}) measurements of extracellular current density immediately above the surface of the opercular membrane. The chamber was placed on the stage of an upright microscope. Transepithelial voltage was measured with a pair of agar bridges (V_m, V_s); current was passed by Ag-AgCl wires (*i*). The baths were continuously perfused (arrows). A reference electrode for the vibrating probe was also in the mucosal bath (*not shown*)

cells without detection of current flow through other chloride cells.

Taking advantage of this capability to sample individual cells, the present study examines the amount of transport variability among individual, presumably nonelectrically coupled, chloride cells within the same tissue and among different tissues. We have analyzed the responses of individual cells to rapid perturbations, including ion replacement and hormonal stimulation, as well as the degree of steady-state variability in short-circuit current and conductance. The results reveal a great deal of transport variability among individual chloride cells. Analysis of this variability suggests that the chloride cell exerts control over the conductance of its paracellular pathways.

Materials and Methods

Tilapia, *Sarotherodon mossambicus*, were maintained and adapted to seawater as previously described (Foskett et al., 1981; 1982*b*). Seawater adaptation times ranged from 2 to 6 weeks prior to experiments. Opercular membranes were dissected as previously described (Foskett et al., 1981) and the connective tissue removed by teasing with fine forceps under microscopic observation.

Experimental Chamber and Solutions

The isolated opercular membrane was mounted in a modified, Ussing chamber which was placed on the stage of a microscope; both sides of the tissue were continually perfused with oxygenated Ringer's solution while it was viewed from above (Fig. 1). The tissue was mounted horizontally across a circular aperture (area = 0.516 cm^2) with the apical side up. Each membrane was supported on a nylon mesh (Nytex HC3-209) and stretched between pins around the aperture. Silicon grease (Dow) was smeared above and below the tissue around the edge of the aperture as a sealant, and a thin annular Lucite® disk was pressed down over the tissue around the edge of the aperture. This disk was made approximately 1 mm thick, to allow the shank of the vibrating electrode to approach the tissue from as nearly a horizontal direction as possible. The mucosal bath was continuously perfused with fresh Ringer's solution by gravity-feed from an overhead reservoir and drained by continuous aspiration. The bottom of the chamber was a coverslip; the tissue and coverslip defined the serosal compartment which also was continuously perfused with Ringer's solution from another overhead reservoir. We eliminated trans-tissue hydrostatic pressure gradients by manipulating the serosal bath outflow resistance.

At the base of the serosal compartment, a chlorided silver wire encircled and cut across the center of the aperture to the outside of the chamber, and served as a current-passing electrode. A similar wire in the mucosal bath encircled the aperture at a greater radius. Voltage scanning with the vibrating probe demonstrated that this geometry insured a uniform current density at the level of the tissue during transepithelial current passage. Separate input ports allowed the tips of agar bridges to be placed within 2 mm of each surface of the tissue. Experiments were carried out under observation by an upright, fixed-stage microscope with differential interference contrast optics (Aus Jena) utilizing 32× (Leitz) and 10× (Zeiss) objectives with working distances 6 and 4.8 mm, respectively. A commercial voltage-clamp circuit was used employing series resistance compensation (Model 710C, Bioengineering Division, College of Medicine, University of Iowa). Transepithelial potential was measured by calomel electrodes connected to the chamber by the agar bridges that ended near the two sides of the tissue. Current was passed by the chlorided silver wires on either side of the tissue. The current-passing electrode on the apical side was held near ground by a virtual ground circuit contained in the voltage clamp.

Vibrating Probe: Construction

The vibrating probe extracellular recording technique was a modification of that described by Jaffe and Nuccitelli (1974). The metal probe electrode was constructed as described in a previous paper (Scheffey et al., 1983). The tip of a metal-filled microelectrode was platinized under microscopic observation using a protocol similar to that of Jaffe and Nuccitelli (1974). Tips of diameter 4 to 6 μm with capacitances of 0.3 to 1 nF were used in the present study. The electrode was vibrated by driving a glass rod (to which the electrode was attached with dental wax) with a piezoelectric bimorph (PZT-5HN, Vernitron Piezoelectric Division, Bedford, Ohio) which was powered with a sine wave of up to 20 V peak-to-peak at a resonant frequency near 1.6 kHz. This vibration allowed the electrode tip to be vibrated along a line up to 20 μm long. In the present study, the height of the probe's center of excursion above the tissue was 7 to 15 μm, and the vibration excursion was 4 to 7 μm, in a direction 20° from vertical.

The reference electrode for the probe was a chlorided silver wire nearby in the bath. The voltage signal was measured by a differential preamplifier with an input capacitance of 20 pF and

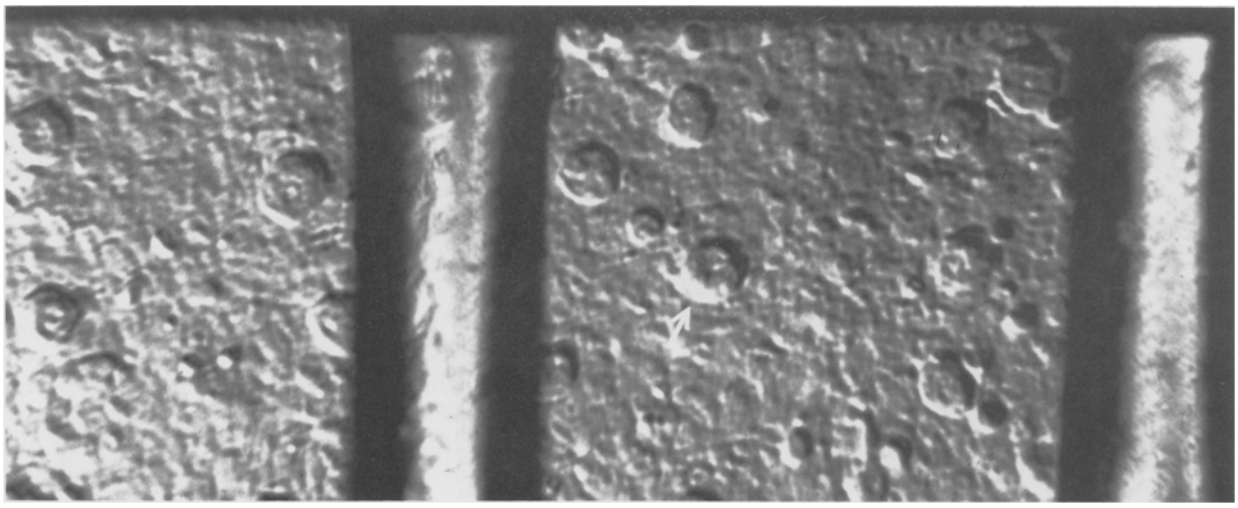

Fig. 2. Light micrograph of opercular membrane mounted in the chamber and voltage-clamped to 0 mV. The supporting nytex mesh (opening = 209 μm) is also shown. Chloride cells (arrow) are large compared with mucous cells and possess "dimples" which are the apical crypts, where contact of these cells with the surface is made

an input noise density was under 6 nV/Hz$^{1/2}$ at the frequency of vibration. The tip could also be connected through a 12 pF capacitor to a 6 mV amplitude triangle wave, for the purpose of measuring tip capacitance and convergence resistance to assure that the tip had not fractured or accumulated excessive debris.

The tip voltage signal from the preamplifier was processed by a lock-in amplifier. The output of the lock-in amplifier was one-pole filtered with a time constant of 0.1 to 0.66 sec; responses to changes in the field were with a time constant equal to that of the output filter. Current noise was within a factor of 2 or the theoretical minimum, typically 1 μA/cm^2 rms.

Vibrating Probe: Calibration

Because the vibration of the electrode tip vigorously stirred the nearby solution (for a detailed description of the flow pattern produced by the probe, *see* Jaffe and Nuccitelli, 1974), it was assumed that the resistivity of the Ringer's near the vibrating probe was the same as the bulk Ringer's resistivity, even when the probe was located near the membrane surface, where ion or water transport might alter the local resistivity in the absence of stirring[1]. With that assumption, lock-in output is proportional to the current density in the line of vibration. The constant of proportionality between the lock-in output and the electric field in the direction of vibration was determined empirically, as described previously (Scheffey et al., 1983).

By using the same geometry for both probe calibration and for measuring the current pumped by individual chloride cells, the estimate of current pumped by the cell was insensitive to error in estimating the direction of probe vibration, which could not be directly observed during the nearly vertical vibration. For measurements conducted in chloride-free Ringer's, the conversion factor from probe signal to current density was obtained by multiplying the conversion factor for normal Ringer's by 0.6, the empirically determined ratio between the conductivities of the two Ringers'.

Scanning Electron Microscopy

Freshly dissected opercular membranes and membranes which had been mounted in the chamber described above and explored with the probe were fixed for 12 hr at room temperature in Karnovsky's fixative containing 1% paraformaldehyde, 2% glutaraldehyde in 0.1 M sodium cacodylate, pH 7.4, supplemented with 4 mM $CaCl_2$. The tissues were washed in 0.1 M sodium cacodylate buffer and postfixed in 1% OsO_4 in cacodylate buffer for 1 hr at room temperature, dehydrated in ethanol and CO_2-critical point dried. Dried samples were sputter-coated with 200 Å of Au-Pd, and viewed with a Coates and Welter SEM.

Solutions

The Ringer's solution had the following composition (in mM): 160 Na, 151 Cl, 15 HCO_3, 3 K, 2 Ca, 1 Mg, 1 SO_4, 5 tris(hydroxymethyl)-aminomethane (Tris), 10 glucose. The pH was adjusted to 7.9 by H_2SO_4 titration when gassed with a 99% O_2/1% CO_2 mixture at 24 to 26°C. Chloride-free Ringer's was obtained by substitution of all chloride with 147 mM isethionate and 4 mM gluconate. Hormone additions were from stock solutions added

[1] The geometry of the apical crypt of a chloride cell precludes stirring the solution immediately adjacent to the chloride cell apical membrane. Since the crypt often contains within it a high concentration of glycoproteinaceous material, it is possible that the resistivity within the crypt is different from that of the solution immediately outside the crypt opening. In the steady state, the amount of chloride current which flows out of the chloride cell is the same as flows through the glycoprotein and into the bulk medium. Thus, as long as the measurement by the probe is made in a medium of *known* resistivity (i.e. above the chloride cell), the steady-state current can be accurately measured.

Fig. 3. Scanning electron micrograph of apical surface of opercular membrane. The opening of what is probably the apical crypt of a chloride cell at the junction of three surface pavement cells is shown. Bar is 5 μm

to the reservoir feeding the serosal compartment. Addition of the phosphodiesterase inhibitor, 3-isobutyl-1-methyl-xanthine (IBMX, Sigma, St. Louis, Mo.) was to both perfusion reservoirs to maximize intracellular penetration (final bath concentration = 100 μM). L-epinephrine and glucagon (both from Sigma) were used at a final concentration of 1 μM.

Results

Figure 2 is a light micrograph of an opercular membrane taken while the tissue was mounted in the chamber described above and perfused on both sides while simultaneously voltage-clamped to 0 mV. Underlying the tissue is a nylon-mesh support. The chloride cells are easily observed against a rather uniform background and can be identified by their large sizes (20 to 40 μM diameter, compared to smaller mucus cells, 5 to 10 μM diameter) and by the small dimples associated with each of them. Although the width of chloride cells when viewed from above is large, each cell makes only a limited contact with the apical solution via a 1 to 3 μm diameter apical crypt (Foskett et al., 1981). This point is emphasized in Fig. 3 which shows a scanning electron micrograph of the apical surface of an opercular membrane. Whereas the surface is largely covered by so-called pavement cells, characterized by fingerprint patterns of microridges, occasional chloride cells make contact with the surface via openings at the junctions of two or three pavement cells.

The small dimples associated with chloride cells observed with the light microscope (Fig. 2) are almost certainly apical crypts since vibrating probe measurements have demonstrated that current flow through these cells is maximum when the probe is positioned over the dimples (Scheffey et al., 1983; this study). The optical quality demonstrated in Fig. 2 was typical for all experiments and permitted accurate positioning of the probe over the cell as well as measurement of the height of the tip of the probe above the tissue. The accuracy of the latter measurement was critical to be able to convert the probe-measured current densities into absolute surface-sources of current, since the conversion is an exponential function of the height (Scheffey et al., 1983; *see also* Eq. (1) below)[2]. It has been demonstrated that the current density measured by the probe is not significantly different from zero within 20 μm from the apical crypt (Scheffey et al., 1983). The combination of high probe spatial resolution and improved optics described here permits electrophysiological studies of individual chloride cells. Thus, transport variability among individual, presumably nonelectrically coupled, chloride cells within the same tissue, as well as among different tissues, could be assessed.

To study steady-state variability and variations in the response to hormonal and ionic perturbations among individual cells, several "cell-sampling" experiments were conducted in which the transport activities of a number of randomly selected chloride cells in each of several tissues were measured with the probe. Figure 4 shows the typical protocol used to measure the individual chloride cell short-circuit current and conductance. The probe output corresponding to zero current density was determined by initially positioning the probe approximately 250 μm above the tissue while the tissue was at open-circuit conditions (Foskett & Scheffey, 1982; Scheffey et al., 1983). The chloride cell current under

[2] The height of the tip of the probe above the tissue surface was determined by the difference in the microscope focus micrometer reading when the focus was on the center of the tip of the probe versus when the focus was on the surface of the tissue. Although most of the work presented here was with a 10X objective with a 0.22 numerical aperture, two sets of preliminary experiments demonstrated that the error in this determination was usually within 15%. The first method compared the distance between the probe and a fixed microelectrode optically and electrically. The second method compared the distance measured optically with that determined by manually lowering the probe and recording its displacement until it touched the epithelial surface (detected as noise on the probe output).

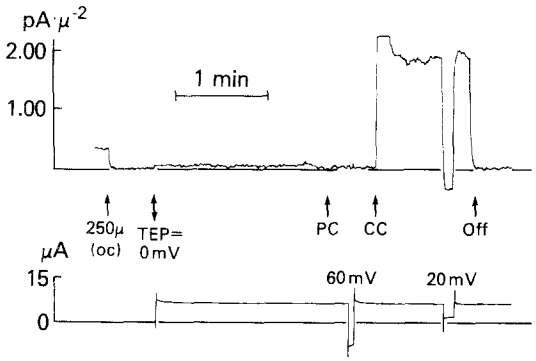

Fig. 4. Typical protocol used to measure short-circuit current and conductance of an individual chloride cell. Upper trace: vibrating probe output (converted to a current density—1.00 pA/cm² corresponds to a probe output of 100 mV); lower trace: tissue short-circuit current. The signal when the probe is positioned 250 μm above the tissue under open-circuit conditions (*oc*) defines the zero-current probe output. At the second arrow the tissue is voltage-clamped to 0 mV (TEP = 0 mV). At the third arrow the probe is lowered to a position 11 μm above a surface pavement cell (*PC*). The probe output is close to that for zero current density. The transepithelial voltage was transiently stepped to 60 mV. The simultaneously measured probe output indicates that these cells have extremely low conductance. At the fourth arrow, the probe was positioned 15 μm above the apical crypt of a chloride cell (*CC*). The transepithelial potential was transiently stepped to 20 mV. The response of the probe output demonstrates that chloride cells are sites of high conductance. The probe vibration was subsequently halted and the height of the probe above the tissue was measured

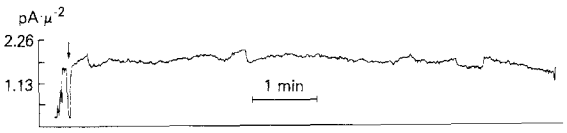

Fig. 5. Continuous record of vibrating probe output for over seven minutes while the probe was positioned over the apical crypt of a chloride cell. The cell conductance was determined at the beginning of the record (arrow) by transiently stepping the transepithelial voltage to 20 mV (serosa positive). 1.13 pA μm^{-2} corresponds to a probe output of 100 mV

short-circuit conditions I_{cc} was determined according to:

$$I_{cc} = \frac{FC}{2}\left(\frac{h}{H}\right)^2 \frac{V_1}{V_2} \quad (1)$$

where V_1 is the probe signal measured at height h over the cell, V_2 is the probe signal measured during calibration in response to passing current C from a microelectrode at height H (typically 100 μm) and F is a correction factor of 0.9 to 1.0 which corrects for the experiments' departures from an idealized geometry (*see* Scheffey et al., 1983). Following stabilization of the probe output over the chloride cell, the transepithelial voltage was rapidly clamped to 20 mV (serosa positive), and the deflection of the probe output was recorded. The current-voltage relation for chloride cells is linear over this range of transepithelial voltages (Foskett & Scheffey, 1982; Scheffey et al., 1983). Thus, the conductance of the chloride cell G_{cc} (which includes both the paracellular and cellular pathways) was calculated according to:

$$G_{cc} = (I_{cc} - I_{cc}^{20})/20 \text{ mV} \quad (2)$$

where I_{cc} is the chloride cell short-circuit current and I_{cc}^{20} is the chloride cell current at a transepithelial voltage of 20 mV. Following measurement of the chloride cell conductance, the vibration of the probe was halted, and the height of the center of the tip of the probe above the surface was measured optically, correcting for the refractive index of the medium. Figure 5 shows a continuous measurement for seven minutes of the short-circuit current through an individual chloride cell. The steady-state short-circuit current generated by the whole tissue is the result of continuous, steady chloride extrusion by each cell, as opposed to discrete on and off episodes. The figure shows that the presence of the probe does not affect the ability of the cell to pump current. As a result, measurements of an individual cell's current and conductance could be made repetitively over time to examine the effects of various perturbations.

Effects of Chloride Removal on *I* and *G* of Individual Cells

The effects of chloride removal from the bathing media on I_{cc} and G_{cc} of six individual chloride cells is shown in Fig. 6. As expected, since the current traversing these cells is carried by chloride (Foskett et al., 1981, 1982*b*), removal of chloride resulted in a reduction of the probe-measured current to near zero over all six cells. The conductance for five of the six cells was also diminished. The response to re-introduction of chloride was less uniform. Although all cells responded with increased current, the degree of recovery was variable. Half of the cells recovered fully, but the other half recovered to less than 50% of the pre-inhibition levels. It is interesting that those cells whose currents were restored to pre-inhibition levels also demonstrated a completely restored conductance. Likewise, cells with unrestored currents had unrestored conductances. This apparent coupling between cell current and conductance was not strict, however, since partial restoration of current can be associated with no

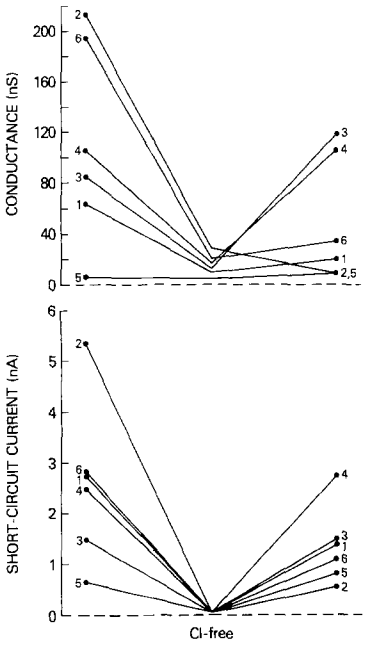

Fig. 6. Effects of chloride removal on short-circuit currents and conductances of six individual chloride cells

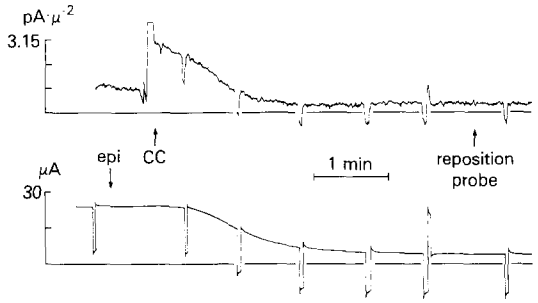

Fig. 7. Time courses of epinephrine inhibition of tissue short-circuit current (lower trace) and individual chloride cell current (probe output; upper trace). Epinephrine (*epi*, 1 μM) was added at first arrow; the probe was placed above a chloride cell (*CC*) at second arrow. Deflections are the result of momentary steps of transepithelial potential from 0 to 20 mV. The tip of the probe was repositioned laterally at the third arrow to maximize the signal, demonstrating that the decline in probe output was not due to probe or cell movement

change or a decrease in conductance, as seen in Fig. 6.

Effects of Epinephrine on I_{cc} and G_{cc} of Individual Cl Cells

Chloride secretion by the opercular membrane can be rapidly modulated by a variety of hormones (reviewed by Foskett et al., 1983). Epinephrine, via α-receptors, blocks chloride efflux and is a fast-acting inhibitor of the short-circuit current in this tissue (Foskett et al., 1982*a*). The typical time course of inhibition (*see* Fig. 1 Foskett et al., 1982*a*) could reflect the time course of inhibition of each cell, or might instead represent the integrated result of cells shutting off instantly, upon epinephrine binding, at different times. To test which possibility was correct, simultaneous measurements of the tissue short-circuit current and individual chloride cell short-circuit currents were made during inhibition by epinephrine. As seen in Fig. 7, the time-course of inhibition observed for the whole tissue is closely paralleled by that for an individual chloride cell. Similar continuous measurements over three chloride cells in as many tissues yielded the same results.

Average inhibition of tissue short-circuit current by 1 μM epinephrine is 60% (Foskett et al., 1982*a*). Even with very high concentrations (10 μM), nearly 20% of the short-circuit current remains, possibly because a subset of the chloride cell population is insensitive to epinephrine. Variability among chloride cells in their responsiveness to epinephrine was examined in several cell-sampling experiments similar in design to that employed in the chloride-free experiments. Figure 8 is a summary of one such experiment. Eight nearby chloride cells were selected, and their currents and conductances measured during control conditions. The tissue was then inhibited with 1 μM epinephrine, and the currents and conductances of the same eight cells were subsequently determined when the tissue short-circuit current was again stable. In the experiment depicted in Fig. 8, epinephrine inhibited the current in all eight chloride cells. Its effect on chloride cell conductance was more variable. In some cells (cells 1, 4, 5), conductance was increased while in others (cells 2, 3, 6, 7), epinephrine decreased it. Phosphodiesterase inhibition by IBMX, and/or exposure to glucagon stimulates short-circuit current in opercular membranes previously inhibited with epinephrine (Foskett et al., 1982*a*). As shown in Fig. 8, IBMX/glucagon restores the current completely in some cells (cells 1, 4, 5, 7), restores it partially in others (cells 3, 6, 7) or has no effect (cell 2). IBMX-glucagon treatment may enhance (cells 1, 3, 6, 7) or decrease (cells 2, 4, 5) cell conductance. The net effect of all these changes is to mimic fairly closely the tissue response (Fig. 8).

The degree of variability among chloride cells in their responsiveness to hormones was similar to that observed in the chloride-free experiments. Unclear, however, was the actual source of this variability. It did not appear to correlate with any morphological parameters (cell size, shape or location,

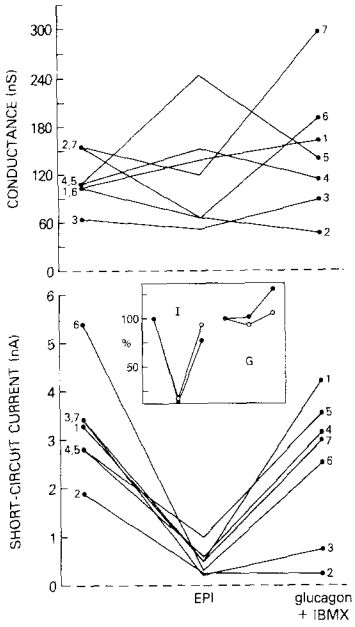

Fig. 8. Effects of epinephrine and subsequent exposure to glucagon and IBMX on short-circuit currents and conductances of seven individual chloride cells in a single tissue. Insert compares responses of the tissue (open circles) with those of the cells (closed circles)

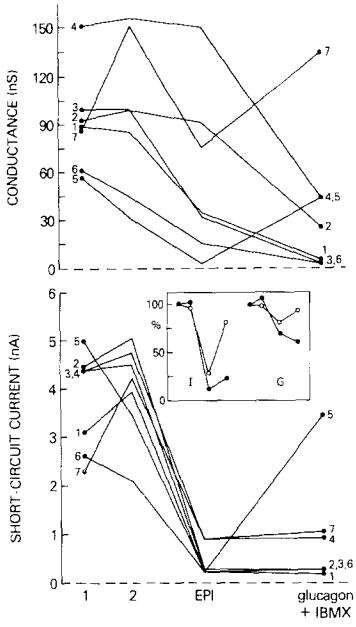

Fig. 9. Effects of epinephrine and subsequent exposure to glucagon and IBMX on short-circuit currents and conductances of seven individual chloride cells in a single tissue. First two measurements over each cell were during control periods separated by 15 to 20 min. Insert compares responses of the tissue (open circles) with those of the cells (closed circles)

or size or location of the apical crypt) although this was not systematically analyzed. The time between sampling periods was usually 15 to 20 min. It was possible that there might have been temporal changes in the current and conductance over this time period, independent of the hormonal treatment. In addition, since the calculation of the amount of current pumped by a cell is critically dependent upon the determination of the height of the probe above the tissue (Eq. 1), it was possible that differences in individual cell electrophysiological parameters between measurements were the result of an inability to accurately measure the height of the probe above the tissue. We therefore undertook another series of cell sampling experiments in which the hormonal perturbations were after two control measurements separated by 15 to 20 min. Figure 9 summarizes such an experiment. In most instances, these are very small differences between the two control measurements. For 43 cells in six tissues, the current and conductance during the second control measurement were 116.1 ± 7.7 and 110.8 ± 7.4%, respectively, of the first measurement values. These data suggest that it is possible to measure accurately and repeatedly the height of the probe above the cell. Sometimes the values in the second control period were clearly different compared to the first period, as for cells 5 and 7 in Fig. 9; however, it is impossible to decide whether the differences between the two periods are due to experimental error or to real changes in the cells.

Clearly, however, epinephrine inhibits the current in all cells examined (Figs. 8 and 9). Of 45 cells examined using this protocol in six tissues, all were markedly inhibited by epinephrine (by 85.7 ± 2.0%; ranging from 31 to 100%). The most striking variability among individual cells is in the response of cell conductance. In the particular experiment shown in Fig. 9, epinephrine ultimately resulted in large decreases in conductance in all seven cells. It is noteworthy that for some cells (cells 2, 4) the effect of epinephrine to inhibit the current preceded any significant effect on the conductance. Glucagon-IBMX were largely without effect on this group of cells, in contrast to their effect on the whole tissue.

Steady-State Transport Variability among Cells

During the course of our studies, we made steady-state measurements of short-circuit current and conductance for 386 chloride cells. Of these, only five failed to generate a measurable short-circuit current. A great amount of variability exists among

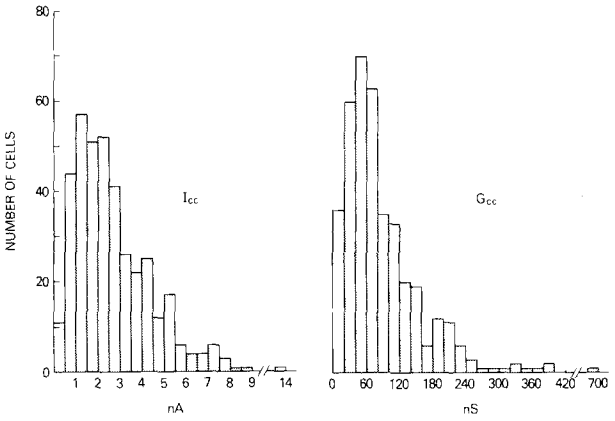

Fig. 10. Histograms showing distributions of steady-state chloride cell short-circuit currents (I_{cc}) and conductances (G_{cc})

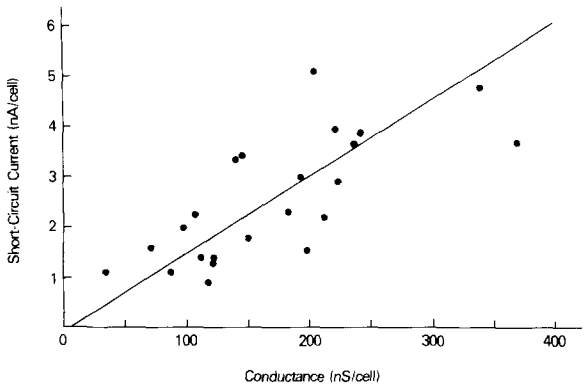

Fig. 11. Relationship between short-circuit current and conductance of individual chloride cells in a single opercular membrane. Line is the best-fit correlation line. Each point represents steady-state values for a single chloride cell

chloride cells in their transport parameters: cell currents ranged from 0 to 14 nA and individual cell conductances from 0 to 697 nS. This variability was not normally distributed for either current or conductance (Fig. 10). The average chloride cell current was 2.7 ± 0.1 nA; the average individual cell conductance was 87.7 ± 3.8 nS.

As well as variability among chloride cells among different tissues, there usually existed a rather wide range of chloride cell currents and conductances within the same tissue. We examined this in some detail in series of experiments in which in each of 10 tissues between 21 and 44 cells were randomly selected and their currents and conductances measured. Figure 11 shows steady-state variability among chloride cells in one of these tissues. The variability among cells within the tissue describes a linear relationship between current and conductance with intercept at zero. Similar relationships were observed in all ten tissues (Table). The possible significance of these relationships will be discussed below.

Discussion

Utility of the Vibrating Probe Technique for Measuring Currents and Conductances of Chloride Cells in the Opercular Membrane

The present results further demonstrate the utility of the vibrating probe technique in the analysis of the transport pathways in heterogeneous epithelia. In our previous studies, we refined this technique to localize a specific cell type as the site of electrogenic chloride secretion in a complex epithelium (Foskett & Scheffey, 1982; Scheffey et al., 1983). We here provide evidence for the chloride cell as a hormone-responsive cell, and demonstrate the degree of variability among individual chloride cells in their responsiveness to rapid perturbations and in their steady-state transport parameters.

The results of the present study suggest that all chloride cells possess functional α-adrenergic receptors. In nearly 50 cells examined, the short-circuit currents in all were substantially reduced by epinephrine. In three tissues the time-course of inhibition of the tissue short-circuit current was found to be a reflection of those of the individual chloride cells. The results also demonstrate that in epinephrine-treated tissues (in which currents are low), glucagon and phosphodiesterase inhibition stimulate the tissue's short-circuit current by reversing the current of most (but not all) of epinephrine-inhibited chloride cells. There were no effects of any hormonal treatment on current and conductance of non-chloride cells (*not shown*).

In the steady state, when short-circuit current and conductance were measured over the same cells at two times, values were within 15% of the first measurements when measured again 15 to 20 min later. This suggests that it is possible to come back to previously examined cells and accurately reposition the tip of the vibrating probe and measure its height above the surface of the epithelium to within 10 to 15%. The ability to make this height measurement accurately is critical since in the present experiments an error of only 1 μm in this determination would lead to a 15% error in the calculation of current and conductance. Accurate repositioning of the probe was possible due largely to the excellent visualization of the chloride cells and their apical crypts with differential interference contrast optics. Whether the optical characteristics

of other tissues also permit such visualization will determine whether repetitive measurements over the same site can be made.

The short-circuit current and conductance of nearly 400 chloride cells were determined, during the course of these studies, and a great deal of variability among chloride cells was observed. Using the average chloride cell current (2.7 ± 0.1 nA) and conductance (87.7 ± 3.8 nS) and assuming a hemispherical apical membrane with a diameter of 3 μm (Foskett et al., 1981), area-specific surface current and conductance for chloride cells are 19 mA cm^{-2} and 620 mS cm^{-2} (resistance = 1.6 Ω cm^2), respectively. Chloride cells thus rank as one of the most actively transporting and conductance cells known. Since the chloride cell paracellular pathway ramifies throughout the apical membrane (Foskett et al., 1983), this area-specific conductance is partitioned between the cellular and associated paracellular pathways. However, the conductance of the chloride cell apical membrane *per se* must be extremely large since the chloride current must traverse it. A minimum estimate can in fact be calculated. If we assume that chloride current through the apical membrane is the only conductance (a conservative assumption) and that there is no backflux of chloride through this pathway (another conservative assumption), then an average chloride flux ratio of 5.8 (Foskett et al., 1982) implies that the measured current is 83% of the current which crosses the apical membrane. If the voltage across the apical membrane is assumed to be −70 mV (inside negative; a typical-to-somewhat-high value for most epithelial cells—a high value will tend to overestimate the resistance), then from Ohm's Law, the resistance of the apical membrane can be estimated as 3 Ω cm^2. If the single-channel chloride conductance is 360 pS, as recently found in a chloride-secreting cultured epithelial cell line (H. Murer, *personal communication*), then the chloride channel density is approximately 10 · μm^{-2}.

Is There a Relationship Between Cellular Transport and Paracellular Conductance of Chloride Cells?

The vibrating probe technique cannot directly allow partitioning of the chloride cell's total conductance into its cellular and paracellular components. When the variability among chloride cells within ten separate tissues was analyzed, we discovered that a linear relationship between short-circuit current and conductance with intercept at zero was described in each tissue. In an attempt to understand the significance of such a linear relationship, we have analyzed this variability by use of simple electrical equivalent circuit (Fig. 12) in which each chloride cell is modeled as a black box consisting of an active transport cellular pathway, which consists of an electromotive force E_{cc}^{Cl} in series with a conductive pathway G_a (which is determined by the conductive properties of the apical and basal cell membranes), and, in addition, a variable leak conductance G_L (which may involve ionic flow through parallel, cellular conductances and also through tight junctions)[3]. The leak conductance has been described as a variable resistor to account for the following observations. First, in a circuit analysis of the opercular membrane, it was concluded that there exists a link between the magnitudes of the chloride cell cellular and leak pathway conductances such that the ratio between them is constant (Foskett et al., 1982*b*). Second, isotopic flux analyses suggest that sodium (a) traverses the opercular membrane through the chloride cell leak pathway and (b) always contributes 40 to 50% of the tissue conductance over the entire wide range of observed conductances (reviewed by Foskett et al., 1983).[4] These data suggest that the leak pathway conductance G_L is somehow linked to the active pathway conductance G_a in such a manner that the ratio between them is fixed, i.e.

Table. Variability among chloride cells in individual tissues[a]

Expt. No.	Range		Slope (mV)	Intercept (nA)	r	n
	I_{cc} (nA)	G_{cc} (nS)				
1	0 –4.1	0–115	31.1	−0.08	0.880	21
2	0.9–5.1	32–364	15.6	−0.11	0.732	23
3	1.0–6.8	9–162	26.7	−0.16	0.652	39
4	0 –4.4	0–91	48.3	−0.004	0.769	37
5	0.7–4.5	34–248	20.5	−0.06	0.836	44
6	0.2–6.5	8–135	46.2	−0.37	0.762	31
7	1.4–7.3	38–117	66.0	−0.68	0.734	21
8	0.1–5.8	2–168	36.7	−0.04	0.832	35
9	0 –8.9	3–95	77.3	−0.46	0.839	26
10	0.3–14.0	15–697	20.5	+0.39	0.894	37

[a] Slope and intercept define the line generate by variability among chloride cells in I_{cc} and G_{cc}; all lines are linear at $P < 0.001$; r is the correlation coefficient; n is the number of chloride cells sampled in each tissue.

[3] Specific information concerning the individual membranes, paracellular pathways or cell interior cannot be derived from such an analysis (Schultz, 1979).

[4] The difference between the total (cellular + paracellular) conductance associated with the typical chloride cell (620 mS cm^{-2}) and the apical membrane conductance calculated in the previous paragraph (330 mS cm^{-2}) indicates that the leak conductance represents approximately 50% of the total cellular conductance, in good agreement with the sodium flux data.

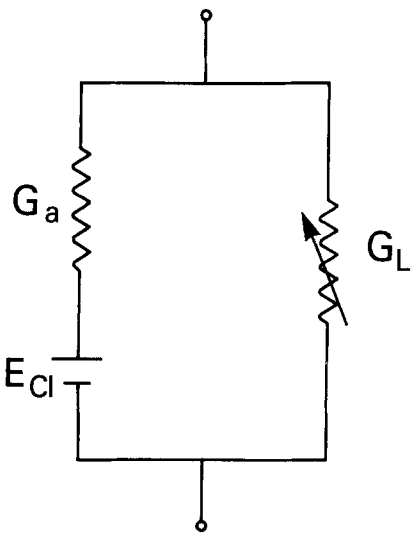

Fig. 12. Simple equivalent circuit for chloride (Cl) transport across chloride cell. Leak conductance (G_L) is linked to the conductance of the active pathway (G_a) such that the ratio between them is constant among cells in each tissue; E^{cc}_{Cl}, chloride driving force (EMF) for chloride cell

$$G_L/G_a = k. \tag{3}$$

In the simple model in Fig. 12, the short-circuit current which flows through such a network due to chloride secretion is

$$I_{cc} = G_a E^{cc}_{Cl}. \tag{4}$$

Since the total conductance associated with a single chloride cell is given by

$$G_{cc} = G_a + G_L \tag{5}$$

it follows that

$$G_{cc} = G_a(1 + k). \tag{6}$$

Therefore, combining Eqs. (4) and (6) and rearranging

$$I_{cc} = G_{cc}[E^{cc}_{Cl}(1 + k)^{-1}]. \tag{7}$$

According to this formulation, if variability in chloride secretion rates among individual chloride cells within a single tissue is caused by cell-to-cell variability in the active pathway conductance G_a, a linear relationship defined by variabilities of G_{cc} and I_{cc} is expected, as observed (Fig. 11; Table). The slope of this relationship is E^{cc}_{Cl} "shorted out" to the extent that the parallel, variable leak conductance G_L contributes to the total cell conductance. To the extent that there also exists another leak conductance which is independent of the active transport pathway conductance, the zero-current G_{cc} intercept will be greater than zero. In all ten experiments presented in the Table, the zero-current intercept was not significantly different from zero, suggesting that all leak conductance associated with a chloride cell is contained within G_L. The most likely interpretation of the linear I_{cc} *vs.* G_{cc} relationship is that a leak pathway is associated with chloride cells, and its magnitude varies in parallel with that of the active transport rate. Chloride cell tight junctions are single- or double-stranded, and sodium fluxes are large ($P_{Na} = 5.2 \times 10^{-4}$ cm sec^{-1}) and appear to be passive and rate-limited by a single barrier (Degnan & Zadunaisky, 1980; reviewed by Foskett et al., 1983). These anatomical and sodium isotopic-flux data are most consistent with the chloride cell tight junctional pathway as the leak pathway.

Thus, the results of the present analysis suggest that in the steady state the chloride cell paracellular pathway "knows" or "senses" the state of the transport activity in the cellular pathway and is modified or adjusted to provide the same relative contribution to the total conductance of each cell within a given tissue. The nature of this control is unknown, but it probably reflects the state of differentiation of the chloride cells in a given tissue, since this relationship is only valid during the long-term steady state, and not after rapid perturbations of transport (Figs. 8 and 9). Chloride cell differentiation is associated with a greatly amplified length per apical membrane area of shallow, single- or double-stranded tight junctions (reviewed by Foskett et al., 1983), and a strong correlation between the size of a chloride cell (another measure of differentiation) and its secretory rate has been noted (Foskett et al., 1981). Thus, increased differentiation of individual chloride cells results in the parallel development of chloride secretory ability and the paracellular pathway, and may constitute the link between the two pathways observed in this study.

We thank Dr. Howard A. Bern for valuable support, advice and encouragement throughout the course of this study, and for his critical reading of the manuscript; Dr. Carl Scheffey for his generous advice; Bobby Taggart, for providing Figure 3; and Drs. Kenneth Spring and Sheldon Miller for carefully reading the manuscript and making many useful suggestions. This investigation was aided by N.S.F. grant PCM-77-25205 and N.I.H grant AM 19520 to T.E.M and by N.S.F. grant PCM 81-10111 and P.H.S. grant CA09041 (awarded by the National Cancer Institute, D.H.H.S.) to H.A. Bern.

References

Degnan, K.J., Zadunaisky, J.A. 1980. Passive sodium movements across the opercular epithelium: The paracellular shunt pathway and ionic conductance. *J. Membrane Biol.* **55:**175–185

Foskett, J.K., Bern, H.A., Machen, T.E., Conner, M. 1983. Chloride cells and the hormonal control of teleost fish osmoregulation. *J. Exp. Biol.* **106:**255–281

Foskett, J.K., Hubbard, F.M., Machen, T.E., Bern, H.A. 1982*a*. Effects of epinephrine, glucagon and vasoactive intestinal polypeptide on chloride secretion by teleost opercular membrane. *J. Comp. Physiol.* **146:**27–34

Foskett, J.K., Logsdon, C.D., Turner, T., Machen, T.E., Bern, H.A. 1981. Differentiation of the chloride extrusion mechanism during seawater adaptation of a teleost fish, the cichlid *Sarotherodon mossambicus*. *J. Exp. Biol.* **93:**209–224

Foskett, J.K., Machen, T.E., Bern, H.A. 1982*b*. Chloride secretion and conductance of teleost opercular membrane: Effects of prolactin. *Am. J. Physiol.* **242:**R380–R389

Foskett, J.K., Scheffey, C. 1982. The chloride cell: Definitive identification as the salt-secretory cell in teleosts. *Science* **215:**164–166

Jaffe, L.F., Nuccitelli, R. 1974. An ultrasensitive vibrating probe for measuring steady extracellular currents. *J. Cell Biol.* **63:**614–628

Karnaky, J.K., Jr., Degnan, K.J., Zadunaisky, J.A. 1977. Chloride transport across the isolated opercular epithelium of killifish: A membrane rich in chloride cells. *Science* **195:**203–205

Marshall, W.S., Bern, H.A. 1980. Ion transport across the isolated skin of the teleost, *Gillichthys mirabilis*. *In:* Epithelial transport in the lower vertebrates. B. Lahlou, editor, pp. 337–350. Cambridge University Press, New York

Scheffey, C., Foskett, J.K., Machen, T.E. 1983. Localization of ionic pathways in the opercular membrane by extracellular recording with a vibrating probe. *J. Membrane Biol.* **75:**193–203

Schultz, S.G. 1979. Application of equivalent electrical circuit models to study of sodium transport across epithelial tissues. *Fed. Proc.* **38:**2024–2029

Received 3 July 1984; revised 16 November 1984